

PREPARATION OF MAGNETITE AND MANGANESE OXIDE IONIC POLYMER NANOCOMPOSITE FOR ADSORPTION OF A TEXTILE DYE IN AQUEOUS SOLUTIONS

A. M. ATTA^{a,b*}, H. A. AL-HODAN^a, S. A. AL-HUSSAIN^c, A. O. EZZAT^a,
A. M. TAWFIK^d, Y. A. EL-DOSARY^c

^a*Surfactants research chair, Chemistry department, college of science, King Saud University, Riyadh 11451, Saudi Arabia*

^b*Petroleum Application Department, Egyptian Petroleum Research Institute, Nasr City 11727, Cairo, Egypt. Fax: 0020222747433; Tel: 0020222747917.*

^c*Department of Chemistry, Faculty of science, Al Imam Mohammad Ibn Saud Islamic University (IMSIU), Riyadh 13318, Kingdom of Saudi Arabia.*

^d*College of Science, King Saud University, Riyadh, Saudi Arabia*

The present work aims to investigate new method to prepare manganese dioxide as well as magnetite nanocomposite based on in-situ technique. The crosslinked copolymeric hydrogel based on 2-acrylamido-2-methylpropane sulfonic acid-co-acrylic acid (AMPS/AA) was used as template to encapsulate the metal oxides by introducing the metal cations followed by redox reaction into the gel networks. The chemical, crystal structures, morphology and metal oxide contents were investigated using different spectroscopy and instrumental analyses. The ability of AMPS/AA metal oxide nanocomposites to remove different concentrations of textile cationic dye water pollutants such as crystal violet (CV) from aqueous environments was investigated using UV-visible measurements. The adsorption measurements confirmed the AMPS/AA metal oxide nanocomposites have high efficiency of to remove 1.5 g/L of CV during short time ranged between 20 and 60 minute. The kinetic study indicated that the adsorption process of CV adsorbate using AMPS/AA metal oxide nanocomposite adsorbents obey chemical adsorption mechanism.

(Received June 16, 2016; Accepted August 20, 2016)

Keywords: Nanocomposites, Manganese dioxide, Magnetite, Textile dyes,
Water pollutants, Adsorbents

1. Introduction

Nanocomposite or hybrid materials are one of the most important functional materials that widely used in membrane technology for water desalination and purification [1-5]. These materials have revolutionized global water treatment strategies because they have better performing desalination, high optimal separation performance, anti-fouling, improved chemical, mechanical, thermal stabilities and higher sustainability among conventional membranes. Thin film nanocomposite (TFN) membranes are produced commercially and used for desalination and water treatments with superior self-cleaning surfaces, tunable separation properties [6-8]. The performance of nanocomposite used for water treatments was affected by type of both polymeric and inorganic nanomaterials used to design these materials [9-11]. The selection of the suitable polymeric and inorganic nanomaterials having unique functionalities as antimicrobial, photocatalytic and superior adsorptive capabilities is very important for design of advanced nanocomposite membranes [11]. The clay, zeolite, silica, magnetic, silver, titania, manganese and zinc oxide nanocomposite polymeric materials achieved good performance for water treatment

*Corresponding author: aatta@ksu.edu.sa

[12-15]. The selection of suitable polymers such as polyamide, acrylates, cellulose, polypeptide, fluorinated, chlorinated and ionic charges polymers played also an effective combined parameters as well as interaction between nanomaterials and polymers for design of high efficient nanocomposites. The water purification performances of nanocomposite materials depend not only on the properties of their individual components but also on their morphological and interfacial characteristics. In-situ synthesis of nanomaterials inside the crosslinked polymers as fibers or sheets became one of the most important preparation methods used to design the effective water treatment nanocomposites [16-20].

In-situ synthesis of nanomaterials is focused on the forming chemical bond between inorganic metal ions and polymers followed by oxidation reduction reactions to obtain homogeneous, control of the nanoscale structures, sizes and shapes nanocomposites [18-20]. The presence of anionic functional groups such as $-\text{SO}_3^{-2}$, and $-\text{COO}^-$, and polar groups such as $-\text{NH}_2$, and $-\text{OH}$ in the polymer networks increase the ability of metal ions to bind the network. The in-situ synthesis procedure has great advantages over other preparation methods to prepare monodisperse metal nanoparticles inside polymer matrixes without forming aggregates [21, 22]. The nanocomposites prepared by in-situ method have great selectivity to absorb the toxic heavy metals from water due to affinity of nano-metal or metal oxide particles to interact with metal ions [23-25]. In the previous works [26-28], in-situ method have been used to introduce iron cations inside 2-acrylamido-2-methylpropane sulfonic acid-co-acrylonitrile (AMPS/AN) crosslinked networks followed by hydrolyzing the iron cations to prepare chemisorbed magnetite nanoparticles to prepare highly adsorbent nanocomposites to treat the industrial waste water. The prepared composites showed high efficiency to absorb heavy metals and organic dyes more than crosslinked copolymers or magnetite nanoparticles. In the present work, copolymeric hydrogel from AMPS and acrylic acid (AMPS/AA) can be used to form magnetite and manganese oxide nanocomposites using in-situ technique. The application of the prepared nanocomposites as adsorbents for organic water pollutant such as crystal violet is another goal of the present work.

2. Experimental

2.1. Materials

2-Acrylamido-2-methyl-1-propanesulfonic acid (AMPS), acrylic acid (AA), N, N'-methylenebisacrylamide (MBA), potassium iodide, ferric Chloride hexahydrate, ammonium hydroxide solution 25%, potassium permanganate and ammonium persulfate (APS) were obtained from Sigma-Aldrich Chemical Co. Different concentrations of crystal violet (CV) solutions were used as water pollutants.

2.2. Synthesis procedures

a) Synthesis of Copolymer Hydrogels

Crosslinked equimolar AMPS /AA copolymers were prepared via radical crosslinking solution polymerization technique using water, MBA and APS as a solvent, crosslinker and initiator, respectively. The AMPS and AA monomers were dissolved in water with the concentration of 75 Volume % in the presence of MBA as a crosslinker (10 wt % based on the total weight of the two monomers). APS was used as initiator (0.1 Wt % based on mol percentages of two monomers). The reaction mixture was bubbled by nitrogen gas for 30 minutes and the reaction temperature raised up to 70°C and the reaction temperature keep constant at this temperature until the formation of the hydrogel. The polymer rods were post cured at 105°C in an air oven for 24 h to ensure complete polymerization and then used for dye removal.

b) Synthesis of magnetite and manganese oxide nanoparticles

Manganese oxide nanoparticles can be prepared by reacting manganese sulfate monohydrate, (3.4 g, 20 mmol) in water (6 ml), with ammonium hydroxide (30 ml). Theses solution was added simultaneously to a hot solution of potassium permanganate (3.8 g, 2.0 mmol; in 30 ml water). The reaction mixture was stirred for 1hr to isolate manganese dioxide as brown precipitate of by ultracentrifuge at 9000 rpm.

Magnetite nanoparticle was prepared by reacting ferric chloride with potassium iodide in the presence of ammonia solution as reported in previous work [29]. Briefly a solution of anhydrous FeCl_3 (4 g; dissolved in 30 mL) was mixed and stirred with potassium iodide (1.32 g, dissolved in distilled water (5 mL) at room temperature with N_2 to keep the mixture oxygen free for one hour. The reaction mixture was filtered and the filtrate was heated at 40 °C under vigorous stirring, then NH_4OH (25%, 20 mL) was added dropwise to the filtrate and the reaction mixture was stirred for another 30 minutes at 50 °C. The Fe_3O_4 nanoparticles were separated from the mixture by ultracentrifugation at 12,000 rpm, washed with water three times and with ethanol two times.

c) Synthesis of polymer composites

Composites with different metal oxides (manganese oxide and magnetite) were prepared by rinsing of AMPS/AA hydrogel in iron or manganese cations solutions until it reached equilibrium from metal cations. Then it was treated with ammonium hydroxide solution after drying from water to form metal oxide inside the network of the hydrogel. In this respect, solutions of ferric chloride (1 g dissolved in 30 mL of distilled water) and KI (0.33 g dissolved in 1.5 ml of distilled water) were stirred for one hour in an oxygen free solution. The filtrate of the reaction mixture was mixed and stirred with dried AMPS/AA hydrogels (0.5 g) at room temperature for 24 h. The AMPS/AA hydrogel was air dried and washed by distilled water and ethanol. The hydrogel was immersed into 100 mL ammonia solution (25 %) and stirred for 3 h to produce insitu magnetite nanocomposites. This procedure was repeated three times to increase metal reloading. The same procedure was repeated to prepare manganese oxide AMPS/AA nanocomposites using the same procedure mentioned above to prepare nanoparticle and nanocomposite.

2.3. Characterization

The chemical structure of the AMPS/AA nanocomposites was elucidated using Fourier Transform infra red spectrometer (FTIR; Nicolet, NEXUS-670).

The surface morphology of the AMPS/AA nanocomposites was observed by scanning electron microscope (SEM; JEOL JXA-840A) instrument at 20 kV.

The crystal structure of AMPS/AA nanocomposites was detected by X-ray powder diffractometer (XRD; Bruker D2 Phaser at 30 kV, 10 mA using Cu anode has $k = 0.15406$ nm at 25⁰ C).

The concentrations of CV in water were investigated before and after mixing with AMPS/AA nanocomposites using double beam UV/vis spectrophotometer (Schimadzu UV-1208 model at $\lambda_{\text{max}} = 590$ nm).

The thermal stability and metal oxide contents of of AMPS/AA nanocomposites were investigated using thermogravimetry analysis (TGA on a Setaram TGA92 instrument at a heat rate of 10 °C/min from room temperature to a maximum temperature of 800 °C under air atmosphere).

2.4. Application of AMPS/AA nanocomposite as adsorbent:

Working aqueous solutions of CV (1, 2, 3, 4, 5 ppm) were used to obtain calibration curve between absorbance and CV concentrations using double beam UV/vis spectrophotometer at a wavelength of 590 nm. Different concentrations of CV (0.5-1.5 g / L) prepared by dissolving in 50 ml DW and stirred with 0.05 g of the composite into a 100 ml conical flask at 25 °C. The filtrate samples were centrifuged and analyzed at different time intervals. The CV concentration was determined at the same wavelength (590 nm). The amount of dye adsorption at equilibrium Q (mg/g) was calculated from the following equation:

$$Q_{\text{max.}} = [(C_o - C_e) \times V / (m)] \quad (1)$$

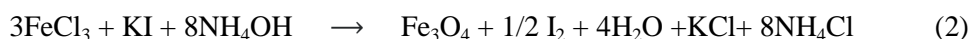
Where C_o and C_e (mg/L) are the liquid phase concentrations of dye at initial and equilibrium, respectively, V (L) the volume of the solution and m (g) is the mass of adsorbent used.

The same procedures to determination of the amount of CV, which adsorbed based on magnetite and manganese oxide composites.

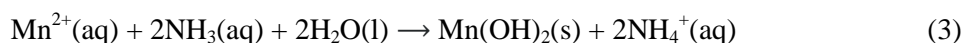
3. Results and discussion

3.1. Chemical structure of nanocomposites

The crosslinked copolymer based on 2-acrylamido-2-methyl propane sulfonic acid and acrylic acid in the presence of MBA crosslinker was selected to prepare nanocomposite due to the presence of different ionic groups such as SO_3H , COOH and weak base amide as represented in Scheme 1. The magnetite can be prepared from reaction of ferric chloride with potassium iodide according to the following equation:



The manganese oxide nanoparticles can be prepared according to the following equations:

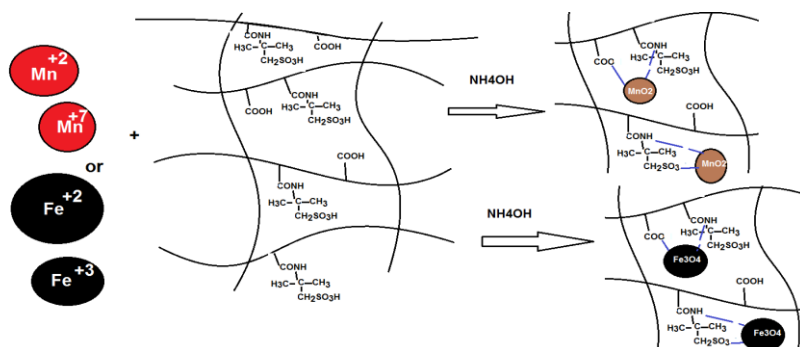


$\text{Mn}(\text{OH})_2$ was oxidized into brown-black MnO_2 in the presence of air(oxygen) and potassium permanganate:



The presence of carboxylic and sulfonic acid groups in the polymer composites assist to use potassium permanganate as very powerful oxidizing agent in which the manganese is reduced from the oxidation state of +7 to +2 with a colour change from purple to colorless (actually extremely pale pink). These groups can interact with iron or manganese cations with noncovalent, covalent bonds or by electrostatic forces between the negatively charged active sites spread throughout the hydrogel and positive charges of iron or manganese cations. It is expected that the iron and manganese cations will penetrate first outside aqueous layer and then the specifically bound water molecules for the sites. Hence, the concentration of adsorbed cations on the hydrogel surface was affected by the water interactions with the hydrophilic groups of AMPS/AA hydrogels. Accordingly, the amount of water sorbed could affect the binding sites and hence, alter the type of interacting forces [30].

The FTIR spectra AMPS/AA, AMPS/AA- Fe_3O_4 and AMPS/AA- MnO_2 nanocomposites were summarized in Figure 1a-c. The characteristic bands of AMPS units exhibit several characteristics bands. The absorption bands at 618 , 1034 cm^{-1} , and 1223 cm^{-1} in all spectra confirm the presence of SO_3 group which referred to the SO stretch, $\text{S}=\text{O}$ asymmetric stretch and symmetric stretch of sulfonic acid groups respectively. The broad absorption band at 3405 cm^{-1} can be attributed to $-\text{OH}$ stretching of carboxylic group of AA. The shifts in the absorption bands at 1613 cm^{-1} 1560 cm^{-1} that referred to amide I mode and amide II confirm the chelation of Mn and Fe of nanocomposites with amide groups of AMPS (Scheme 1).



Scheme 1: In-situ synthesis of metal oxide nanocomposite.

The lowering value of transmittance for sulphonic, amide carbonyl and hydroxyl groups also confirm the chelation of metal cations with AMPS/AA which attributed to the decrease in the dipole moment of SO_3H , CONH and COOH groups as a result of electron donation on the metal ion from the sulfur, nitrogen, and oxygen atoms. The presence of MnO_2 particles can be determined from the appearance of two bands in the finger print region at 515 and 480 cm^{-1} correspond to the Mn-O bond (Figure 1b). The appearance of these two bands indicates that the synthesized nanomaterial inside the AMPS/AA composite is manganese oxide [31, 32]. The type of iron oxide inside the nanocomposite was confirmed from the appearance of new bands at 584 and 637 cm^{-1} assigned to stretching and torsional vibration modes for Fe-O of the magnetite which elucidate the formation of magnetite nanomaterials inside the AMPS/AA composite [33, 34].

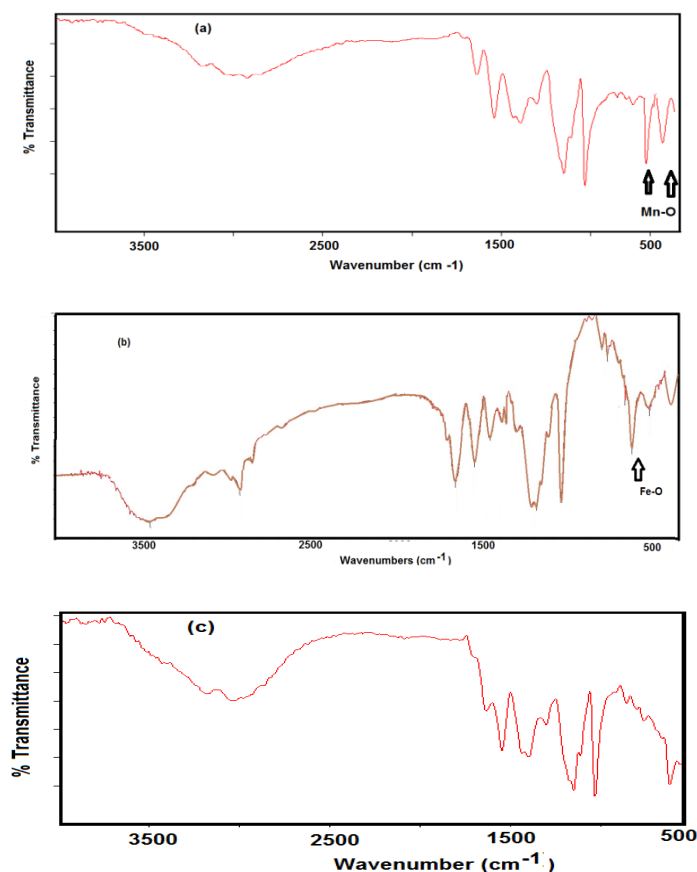


Fig. 1: FTIR spectra of a) AMPS/AA- MnO_2 , b) MPS/AA- Fe_3O_4 and c) AMPS/AA nanocomposites.

3.2. Characterization of nanocomposites

It is expected that there are different types of iron and manganese oxides could be obtain after hydrolyzing their cations. It was reported that, different types of iron oxide such as magnetite, maghemite and hematite during the formation or oxidation of magnetite nanoparticles [29]. Moreover, there are different types of manganese oxides could be produce during the formation of manganese oxides such as α -, β -, γ - MnO_2 and other oxides (Mn_2O_3 or Mn_3O_4) [35, 36]. XRD is an effective tool used to investigate the metal oxides. In this respect, the XRD diffractograms of AMPS/AA- Fe_3O_4 and AMPS/AA- MnO_2 nanocomposites were represented in Figure 2 a and b, respectively. The formation of composites is confirmed from the presence of broad peaks at 2 -theta from 10 to 25° that elucidated the amorphous structure of AMPS/AA copolymers. Moreover, the diffraction pattern and splitting planes of AMPS/AA elucidate that pure cubic magnetite and

orthorhombic α - MnO_2 nanocomposites are produced according with JCPDS card no. 00-002-1035 and JCPDS card PDF file no. 44-0141, respectively with no other impurity peaks [29, 37].

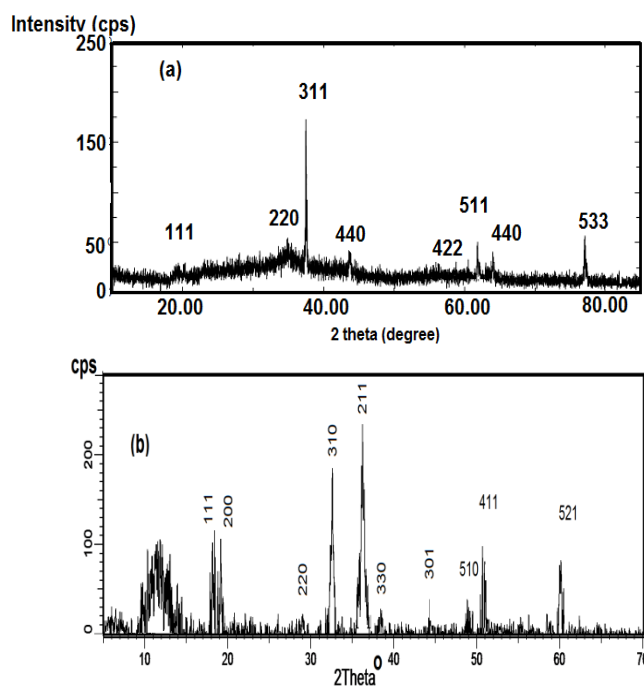


Fig. 2: XRD diffractograms of a) MPS/AA- Fe_3O_4 and b) AMPS/AA- MnO_2 nanocomposites.

The content of MnO_2 and Fe_3O_4 of AMPS/AA- MnO_2 and AMPS/AA- Fe_3O_4 nanocomposites can be determined from TGA thermograms at temperature above 600 °C as illustrated in Fig. 3 a and b.

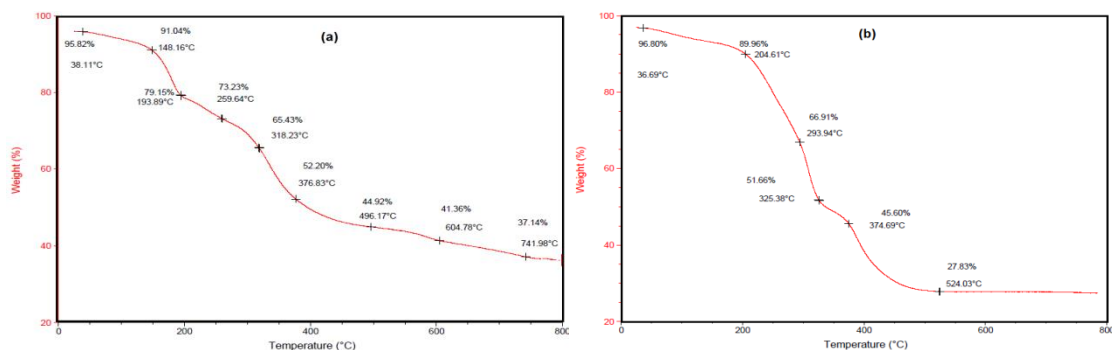


Fig. 3: TGA thermograms of a) MPS/AA- Fe_3O_4 and b) AMPS/AA- MnO_2 nanocomposites.

The data indicated that AMPS/AA copolymers were completely decomposed at temperature of 450 °C. The thermograms indicate that the decomposition of nanocomposites occurred in three steps. The dehydration step started at temperature range 100–190 °C. In the second step, decomposition of AMPS/AA started after 230 °C and continued up to 480 °C. The contents of Fe_3O_4 and MnO_2 were determined at temperature above 750 and 524 °C, respectively (Figure 3 a and b) and they are 37.14 and 27.83 %, respectively.

The surface morphology of AMPS/AA, AMPS/AA- MnO_2 , AMPS/AA- Fe_3O_4 , MnO_2 and Fe_3O_4 nanoparticles and nanocomposites was investigated from SEM micrographs that represented in Figure 4 a and e. The crosslinked AMPS/AA copolymers showed layered skin morphology (Figure 4 a). The presence of magnetite in the polymer AMPS/AA composite was elucidated from

spherical black dots that distributed without aggregates (Figure 4b). The magnetite nanoparticles (Figure 4 c) showed cubic morphology and presence of some aggregates. The MnO_2 particles (Figure 4 d) are almost spherical with uniform particle sizes. The AMPS/AA- MnO_2 nanocomposite (Figure 4 e) has non-uniform distribution with the formation of aggregates. It is expected that the surface morphologies affect the application of the prepared AMPS/AA- MnO_2 , AMPS/AA- Fe_3O_4 , MnO_2 and Fe_3O_4 nanoparticles and nanocomposites as adsorbent to remove toxic dye from water.

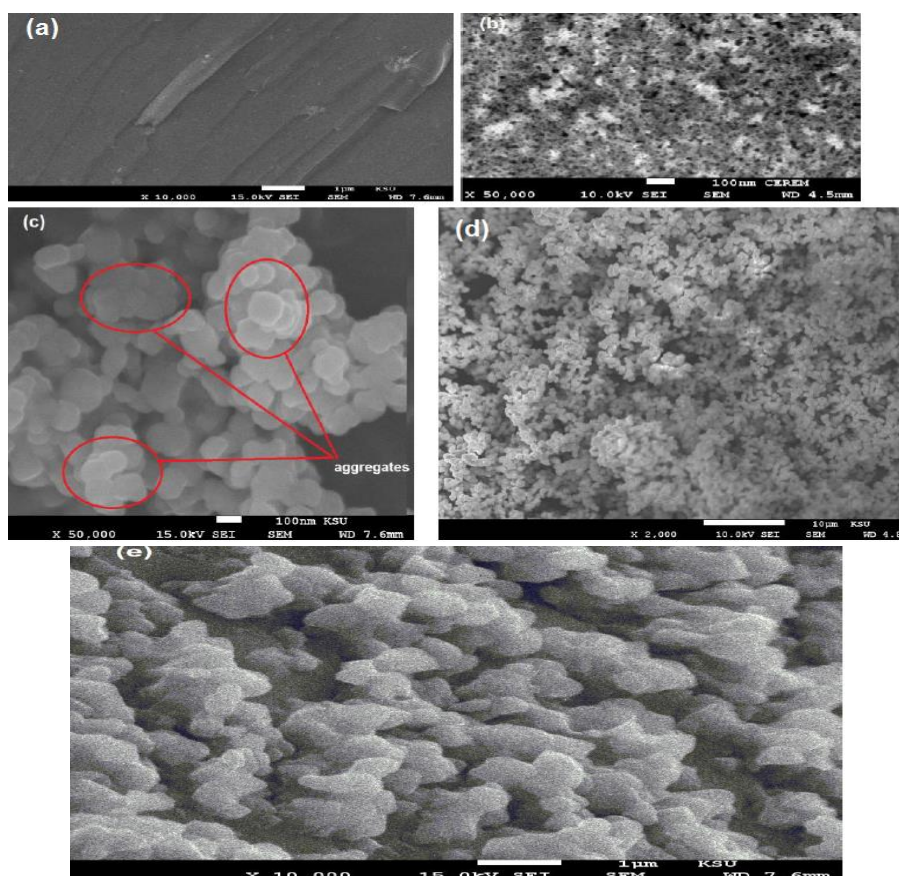


Fig. 4: SEM micrographs of a) AMPS/AA, b) AMPS/AA- Fe_3O_4 , c) Fe_3O_4 , d) MnO_2 , and e) AMPS/AA- MnO_2 nanocomposites.

3.3. Application of nanocomposite

Crystal violet (CV) as cationic dye is one of the serious environmental problems when it discharged in aqueous environments due to its high toxicity as the carcinogenic substances and low biodegradability in such environments [38]. Nanocomposites as adsorbents have been found to be a promising and advancing technique due to simplicity, ease of adsorption, high efficiency, insensitive to toxic environments and low cost-efficiency to remove the organic dyes [39]. In the present work, magnetite nanocomposite was applied as adsorbent to remove the CV from water due to its good bioactivity and magnetic properties that assist to collect the adsorbent after removing the pollutants. The manganese dioxide nanocomposite also used as adsorbent due to its high bio-activity and surface area along with functional groups. Moreover, AMPS/AA hydrogel was selected due to its hydrophilicity, non-toxicity, ionic character and availability. The relation between maximum metal uptake Q_{max} (mg/g) and uptake time (minute) was determined at different concentrations of CV ranged from 0.5 to 1.5 g/L in aqueous system and plotted in Figure 5a-c. Careful inspection of data illustrated in Figure 5 (a-c) confirmed that the fast adsorption of CV occurred at initial time ranged between $t = 0$ and 20 min, and a slower adsorption occurred after this time to reach the equilibrium. The pH and temperature of the aqueous solution were 7

and 298 K, respectively. The results indicated the Q_{max} of hydrogel and hydrogel composites have the same values at 0.5 g/L. While higher adsorption capacity of nanocomposite more than AMPS/AA hydrogel was observed at CV concentration more than 0.5 g/L. The high adsorption capacity of AMPS/AA hydrogel at low CV concentration was referred to electrostatic attraction between anionic sulfonate, carboxylate groups and positive charges of cationic CV dye. The presence of metal oxides nanocomposites in the polymer networks increases the anionic character of AMPS/AA due to chelation of Fe_3O_4 and MnO_2 with the amide groups of AMPS/AA hydrogel [40]. The data (Figure 5 a-c) showed that the AMPS/AA nanocomposites remove the CV pollutant from water during time ranged from 25 to 50 minute. The rapid adsorption of CV onto AMPS/AA nanocomposite can be attributed to the sufficient exposure of adsorptive sites and the high surface reactivity of the adsorbent for sequestering dye anions [41].

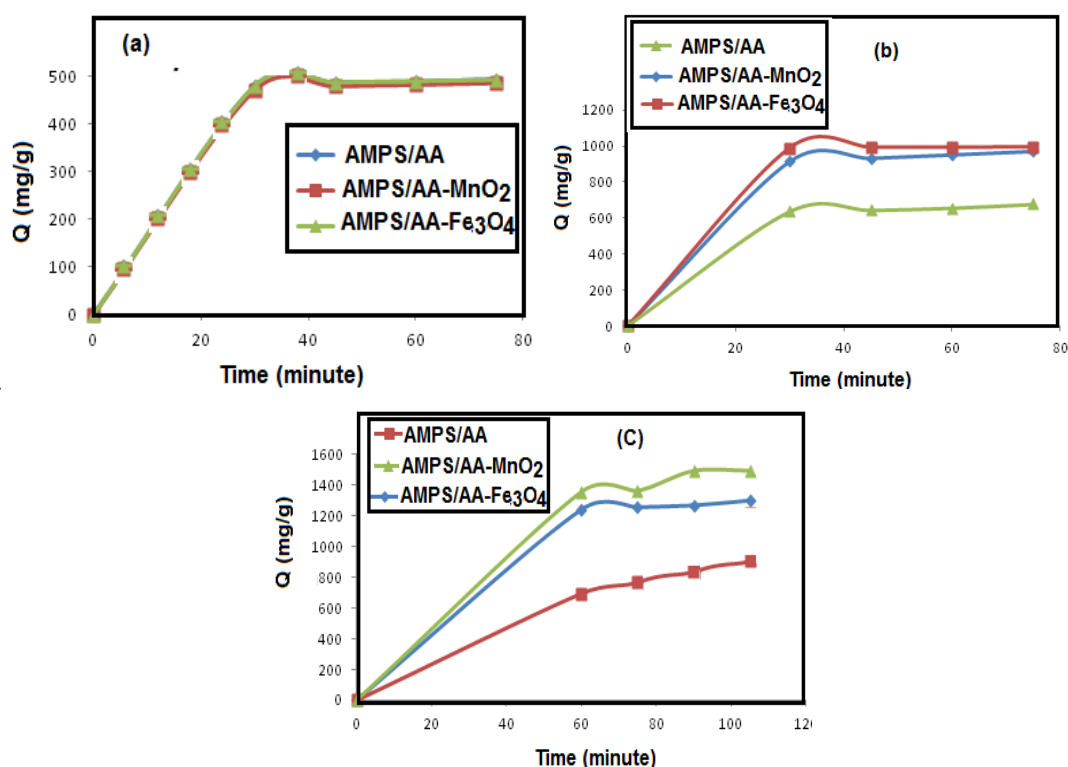


Fig. 5. Relation between Q_{max} (mg/g) and time (minute) of AMPS/AA nanocomposites using different concentrations of CV a) 0.5, b) 1 and 1.5 g/L of CV at 298 K.

It is very important to investigate the adsorption kinetics of the adsorbate (CV) on the adsorbents AMPS/AA composites to detect the nature of adsorption process either, physical, physico-chemical or chemical adsorption. In this respect, pseudo-first-order and pseudo-second order models are used. The rate expression of the pseudo-first-order can be determined from the relation of Lagergren [42, 43] as:

$$\ln(q_e - q_t) = \ln q_e - k_1 t \quad (5)$$

Where q_t and q_e are the adsorption capacity (mg/g) of AMPS/AA composites for CV dye at different times t and equilibrium, respectively. The adsorption rate constant k_1 (min^{-1}) was used to determine the velocity of adsorption process.

The model of pseudo-second-order kinetic is based on the assumption of chemisorption of the adsorbate on the adsorbents and can be expressed as [44, 45]:

$$(t/q_t) = [(1/k_2 q_e^2) + t (1/q_e)] \quad (6)$$

The pseudo- first and second order rate constant k_1 (min^{-1}) and k_2 ($\text{g mg}^{-1} \text{min}^{-1}$) can be determined from the slop of the straight-line plots of the plotting of $\ln(q_e - qt)$ versus t for the pseudo-first-order reaction and t/qt versus t for the pseudo-second order reaction for adsorption of CV onto AMPS/AA composites as illustrated in Figure 6 a-c. The rate parameters k_1 , k_2 , q_e , Q_{max} . and correlation coefficients, r^2_1 and r^2_2 were determined from the plots and summarized in **Table 1**.

It was found that the linear plots via agreements between the experimental Q_{max} . and q_e values occurred for AMPS/AA composites for pseudo-second-order kinetic model. It can be concluded that it is probable that, the CV adsorbed chemically on the active site of AMPS/AA composites.

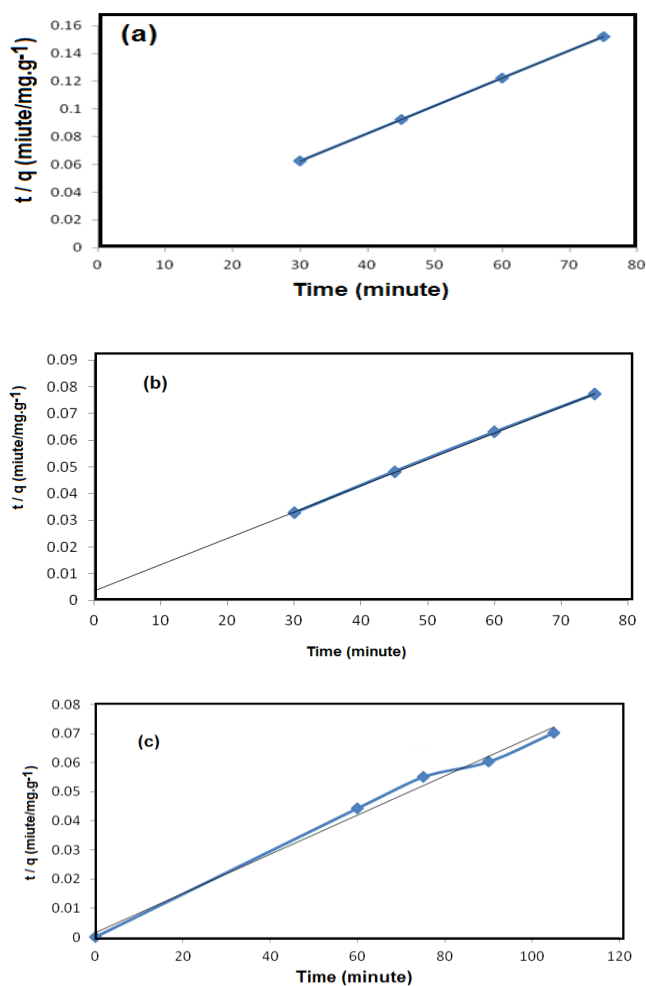


Fig. 6: Pseudo-second order kinetics of AMPS/AA-MnO₂ nanocomposites using different concentrations of CV a) 0.5, b) 1 and 1.5 g/L of CV at 298 K.

Table 1: Kinetic parameters for the adsorption of CV onto AMPS/AA nanocomposites.

Polymer composite	CV concentration (g/L)	Q _{max.} (mg/g) Experimental	pseudo-first-order parameters			pseudo-second-order parameters		
			K1 (min ⁻¹) x 10 ²	q _e (mg/g)	r ₁ ²	K2 (g. mg ⁻¹ . min ⁻¹) x10 ³	q _e	r ₂ ²
AMPS/AA	0.5	500	2.23	577	0.989	1.33	500	1
	1.0	600	2.88	697	0.929	2.0	800	1
	1.5	820	0.9	756	0.922	0.9	1050	0.999
AMPS/AA-MnO ₂	0.5	500	4.3	605	0.972	1.48	500	1
	1.0	950	2.66	721	0.962	2.86	1000	1
	1.5	1500	10.34	1064	0.833	0.3	1428	0.992
AMPS/AA-Fe ₃ O ₄	0.5	500	5.58	659	0.888	1.25	500	1
	1.0	1000	2.29	692	0.866	1.5	987	0.9985
	1.5	1200	4.5	971	0.926	0.8	1110	0.789

4. Conclusions

The carboxylic and sulfonic acid groups in the AMPS/AA polymer were used to carry out redox reaction to produce metal oxide nanocomposites based on Fe₃O₄ and MnO₂. XRD analyses confirmed that the pure α-MnO₂ and magnetite were formed inside crosslinked AMPS/AA polymer composites. It was also found that the Fe₃O₄ and MnO₂ contents are 37.14 and 27.83 %, respectively encapsulate inside AMPS/AA polymer networks. The adsorption measurements confirmed the AMPS/AA metal oxide nanocomposites have high efficiency of to remove 1.5 g/L of CV during short time ranged between 20 and 60 minute. The kinetic study indicated that the adsorption process of CV adsorbate using AMPS/AA metal oxide nanocomposite adsorbents obey chemical adsorption mechanism.

Acknowledgement

The authors would like to extend their sincere appreciation to the Deanship of Scientific Research at king Saud University for its funding this Research group NO (RGP-235).

References

- [1] C. Sanchez, B. Julia'n, P. Belleville, M. Popall, J. Mater. Chem. **15**, 3559 (2005).
- [2] Q. Zhang, X. Li, Y. Zhao, L. Chen, Appl. Clay Sci. **46**, 346 (2009).
- [3] N. Sahiner, Prog. Polym. Sci. **38**, 1329 (2013).
- [4] R.J.B. Pinto, P.A.A.P. Marques, A.M. Barros-Timmons, T. Trindade, C.P. Neto, Compos. Sci., Technol., **68**, 1088 (2008).
- [5] H. Kas, A. Durmus, A. Kas, Polym. Adv. Technol. **19**, 213 (2008).
- [6] R.J. Moon, A. Martini, J. Nairn, J. Simonsenf, J. Youngblood, Chem. Soc. Rev. **40**, 3941 (2011).
- [7] R. Sancha, J. Bajpai, A.K. Bajpai, J. Appl. Polym. Sci., **118**, 1230 (2010).
- [8] J. Liu, S.Z. Qiao, Q.H. Hu, G. Qing, (Max) Lu *small, 7: 425 (2011).

- [9] Z. Xu, C. Li, X. Kang, D. Yang, P. Yang, Z. Hou, J. Lin, *J. Phys. Chem. C* **114**, 16343 (2010).
- [10] C. Sanchez, B. Jul'án, P. Belleville, M. Popall, *J. Mater. Chem.* **5**, 3559 (2005).
- [11] J. Yin, B. Deng, *J. Memb. Sci.* **479**, 256 (2015).
- [12] Y.Q. Rao, J.M. Pochan **40**, 290 (2007).
- [13] Y.M. Mohan, K. Vimala, V. Thomas, K. Varaprasad, B. Sreedhar, S.K. Bajpai, K.M. Raju, *J. Colloid Interface Sci.* **34**, 273 (2010).
- [14] I. Gehrke, A. Geiser, A. Somborn-Schulz, *Nanotechnol Sci Appl.* **8**, 1 (2015).
- [15] R. Li, L. Zhang, P. Wang, *Nanoscale*, **7**, 17167 (2015).
- [16] M.S. Rama, S. Swaminathan, *Ind. Eng. Chem. Res.* **49**, 2217 (2010).
- [17] N. Sahiner, *Colloid Polym. Sci.* **285**, 283 (2006).
- [18] M. Oliveira, A. V. Machado, *Preparation Of Polymer-Based Nanocomposites By Different Routes*, NOVA Publishers, 1-22 (2013)
- [19] S.A. Bencherif, N.R. Washburn, K. Matyjaszewski, *Biomacromol.* **10**, 2499 (2009).
- [20] N. Sahiner, H. Ozay, O. Ozay, N. Aktas, *Appl. Catal. B* **101**, 137 (2008).
- [21] O. Metin, S. Ozkar, *J. Mol. Catal. A: Chem.* **295**, 39 (2008).
- [22] O. Ozay, A. Akcali, M.T. Otkun, C. Silan, N. Aktas, N. Sahiner, *Colloids Surf. B* **79**, 460 (2010).
- [23] O. Ozay, S. Ekici, Y. Baran, S. Kubilay, N. Aktas, N. Sahiner, *Desalination* **260**, 57 (2010).
- [24] N. Sahinera, H. Ozaya, O. Ozaya, N. Aktas, *Appl. Catal. A General* **385**, 201 (2010).
- [25] O. Ozaya, S. Ekicia, Y. Barana, N. Aktasb, N. Sahinera, *Water research* **43**, 4403 (2009).
- [26] Z.F. Akl, S.M. El-Saeed, A.M. Atta, *J. Ind. Eng. Chem.* **34**, 105 (2016).
- [27] A.M. Atta, H.A. Al-Lohedan, A.O. Ezzat, Z. Eissa, A.B. Oumi, *J. Polym. Res.* **23**(4), 69 (2016).
- [28] A.M. Atta, H.A. Al-Lohedan, Z.A. AlOthman, A.A. Abdel-Khalek, A.M. Tawfeek, *J. Ind. Eng. Chem.* **31**, 374 (2015).
- [29] A.M. Atta, H.A. Al-Lohedan, S.A. Al-Hussain, *Molecules* **19**(7), 11263 (2014).
- [30] A.M. Atta, H.A. Al-Lohedan, Z.A. AlOthman, A.M. Tawfeek, A. AbdelGhafar, N.A. Hamad, *Int. J. Electrochem. Sci.* **11**, 3786 (2016).
- [31] L. Kang, M. Zhang, Z.H. Liu, K. Ooi, *Spectrochim. Acta. A* **67**, 864 (2007).
- [32] L. Li, Y. Pan, L. Chen, G. Li, *Solid State Chem.* **180**, 2896 (2007).
- [33] M. Ma, Y. Zhang, W. Yu, H. Shen, H. Zhang, N. Gu, *A : Physicochem. Eng. Aspects* **212**, 219 (2003).
- [34] G.A. El-Mahdy, A.M. Atta, H.A. Al-Lohedan, *J. Taiwan Inst. Chem. Eng.* **45**(4), 1947 (2014).
- [35] D. Yu, J. Yao, L. Qiu, Y. Wang, X. Zhang, Y. Feng, H. Wang, *J. Mater. Chem. A* **2**, 8465 (2014).
- [36] H.E. Wanga, D. Qian, *Mater. Chem. Phys.* **109**, 399 (2008).
- [37] L. Feng, Z. Xuan, H. Zhao, Y. Bai, J. Guo, C. Su, X. Chen, *Nanoscale Res. Lett.* **9**(1), 290 (2014).
- [38] P. Monvisade, P. Siriphannon, *Appl. Clay Sci.*, **42**, 427 (2009).
- [39] S. Karaca, A. Gürses, M. Açıkyıldız, M. Ejder, *Microporous and Mesoporous Mater.* **115**, 376 (2008).
- [40] L. Zhou, J. Jin, Z. Liu, X. Liang, C. Shang, *J. Hazard. Mater.*, **185**, 1045 (2011).
- [41] J.C. Zuo, S.R. Tong, X.L. Yu, L.Y. Wu, C.Y. Cao, M.F. Ge, W.G. Song, *J. Hazard. Mater.*, **235-236**, 336 (2012).
- [42] S. Lagergren, *Handlingar* **24**, 1 (1898).
- [43] Y.S. Ho, G. McKay, *Chem. Eng. J.* **70**, 115 (1998).
- [44] V.C. Srivastava, I.D. Mall, I.M. Mishra, *Chem. Eng. Process.* **47**, 1275 (2008).
- [45] Y.S. Ho, G. McKay **34**, 451 (1999).